are observed during the faster process of shape corrections, that is, for smaller t_f.

IV. Conclusions

A novel mathematical model, computer simulations, and experimental verifications of minimum vibrations that occur during a static shape control using glued collocated piezoelectric actuator/multichannel fibre-optic sensor pairs is presented. The essence of the approach consists in the application of an optimum voltage profile obtained off-line by use of Pontryagin's principle. The applied optimum voltage profile produced the desired shape modification with negligible vibration of the structure as predicted by the simulation.

The results obtained from the optimum control technique have been compared with those of other admissible control profiles. The experimental and simulation results demonstrated that the developed Pontryagin's principle technique creates minimum transient and residual vibrations and allow faster shape correction maneuvers.

References

[1]Crawley, E. F., and Anderson, E. H., "Detailed Models of Piezoceramic Actuation of Beams," *Journal of Intelligent Materials, Systems, and Structures,* Vol. 1, Jan. 1990, pp. 4–25.

[2]Kalaycioglu, S., and Misra, A., "Approximate Solutions for Vibrations of Deploying Appendages," *Journal of Guidance, Control, and Dynamics*, Vol. 14, No. 2, 1991, pp. 287–293.

[3]Kalaycioglu, S., Giray, M. M., and Asmer, H., "Vibration Control of Flexible Manipulators Using Smart Structures," *Journal of Aerospace Engineering*, ASCE, Vol. 2, No. 3, 1998, pp. 90–94.

Spacecraft Formation Flying: Dynamics and Control

Vikram Kapila*
Polytechnic University, Brooklyn, New York 11201
Andrew G. Sparks†
U.S. Air Force Research Laboratory, Wright–Patterson Air Force Base, Ohio 45433-7521
James M. Buffington‡
Lockheed Martin Tactical Aircraft Systems, Fort Worth, Texas 76101
and
Qiguo Yan§
Polytechnic University, Brooklyn, New York 11201

I. Introduction

A NOVEL concept of distributing the functionality of large spacecraft among smaller, less expensive, cooperative spacecraft is seriously being considered for numerous space missions (see also http://www.vs.afrl.af.mil/factsheets/TechSat21.html).[1] A practical implementation of the concept relies on the control of relative distances and orientations between the participating spacecraft. A ground-based command and control system for relative positioning of multiple spacecraft will be excessively burdened and complex and may not be able to provide sufficiently rapid corrective control commands for formation reconfiguration and collision avoidance. Thus, the concept of autonomous formation flying of spacecraft clusters is vigorously being studied by numerous researchers. In particular, NASA and the U.S. Air Force have identified multiple spacecraft formation flying (MSFF) as an enabling technology for future missions. NASA has shown a keen interest in the development of a reliable autonomous formation keeping strategy to deploy multiple spacecraft for deep space missions, e.g., the Earth Orbiter-I and the New Millennium Interferometer (NMI), also known as Deep Space-3. In addition, the U.S. Air Force's TechSat-21 seeks to push the frontier in microscale MSFF to enable global awareness and rapid access to space in the 21st century.

A number of space missions necessitate MSFF. For example, docking of the space shuttle with a space station requires spacecraft rendezvous where it is necessary to fly two spacecraft in close formation in order to capture and dock at the specified time with zero relative velocity. Similarly, spacecraft recovery and servicing missions rely on MSFF. Applications of MSFF to a ground-based terrestrial laser communication system are discussed in Ref. 2, whereas station keeping for the Space Shuttle Orbiter is mentioned in Ref. 3. In recent years Ref. 4 considered MSFF for NASA's NMI, which relies on separated spacecraft interferometry, whereas an MSFF-based stereo imaging concept is discussed in Ref. 5. Finally, in the next millennium the U.S. Air Force's TechSat 21 is expected to provide diverse capabilities, including reconfigurable instantaneous synthetic aperture radar, sensor data fusion from multiple platforms for stereo imaging, theater-wide surveillance, all weather operation and performance, etc., leading to the U.S. Air Force mission of global virtual presence.

Most prior missions requiring MSFF have been carried out using manual flight control[6] and have been limited to one-leader-one-follower configuration. In the case of formation flying of clusters of multiple spacecraft, collision avoidance becomes a significant issue for which ground/manual control may not be reliable. Thus, the development of autonomous formation control strategies is critical to the success of MSFF. Even though the concept of autonomous MSFF has not been flight tested yet, several theoretical and simulation studies dealing with MSFF have been reported in the literature.[2–5,7] In particular, in previous research the nonlinear spacecraft relative position dynamic equations have been developed and linearized[2,8–10] to obtain the Clohessy–Wiltshire (C-W) equations.[9] Furthermore, an impulsive control-based, discrete-time, spacecraft relative position dynamic model and linear quadratic (LQ) regulation technique have been derived in Ref. 2. This methodology has been extended to nonzero set-point tracking control using a combination of feedback and feedforward control techniques.[3] An alternative control scheme using an on-off phase-plane controller can provide ease of implementation. One such algorithm using differential drag elements for actuation is reported in Ref. 11. Latest advances in the phase-plane control design are reported in Ref. 12. Recently, a Lyapunov-based MSFF control design framework has been developed in Ref. 7, which considers absolute attitude alignment and relative translational motion control.

To minimize fuel consumption in MSFF, Refs. 2 and 3 have proposed the use of sample-data, full-state feedback impulsive control schemes. Specifically, a discrete-time model for the linearized spacecraft relative position dynamics has been derived in Ref. 2, assuming that the control is applied impulsively at the sampling instant (as opposed to the standard zero-order, sample-and-hold technique where the control is held constant over the entire sampling interval[13]). However, the approach of Refs. 2 and 3 fails to provide rigorous, a priori guarantees of the closed-loop system stability. This technique also fails to take advantage of recent developments in propulsion technologies. In particular, high-performance Hall thrusters, pulse plasma thrusters, etc., are currently being developed to meet the requirements for future MSFF missions.[14] These low-weight, high-performance thrusters are expected to provide continuous thrusting capabilities for short time intervals, several times every day (if necessary). These advancements in propulsion technologies necessitate the development of novel pulse-based, spacecraft relative position and orientation control laws. In this Note we

Received 29 April 1999; revision received 29 November 1999; accepted for publication 13 January 2000.

*Assistant Professor, Department of Mechanical, Aerospace, and Manufacturing Engineering; vkapila@duke.poly.edu.

†Aerospace Engineer, AFRL/VAAD, 2210 Eighth Street, Suite 21; Andrew.Sparks@va.wpafb.af.mil.

‡Senior Specialist, Flight Control/Vehicle Management Systems, P.O. Box 748; james.m.buffington@lmco.com.

§Graduate Student, Department of Mechanical, Aerospace, and Manufacturing Engineering; qyan01@utopia.poly.edu.

develop pulse-based, discrete-time feedback control laws. Specifically, we design full-state feedback controllers that ensure closed-loop stability in the presence of pulse-type actuators. Before proceeding with the development of pulse-based control scheme, in the next section we review the modeling of spacecraft relative position dynamics.

II. Spacecraft Relative Position Dynamic Modeling

In this section we begin with the classical C-W equations[9] that describe the motion of a follower spacecraft relative to a leader spacecraft. To present the C-W equations, we assume that 1) the leader spacecraft is in a circular orbit around the Earth with an angular velocity ω and 2) a rectangular moving coordinate frame is attached to the leader spacecraft with the x axis pointing opposite to the instantaneous tangential velocity of the leader spacecraft, the y axis pointing along the instantaneous position vector from Earth center to the leader spacecraft, and the z axis is mutually perpendicular to the x and y axis and x-y-z form a right-handed coordinate frame. Thus, it follows that the z axis is perpendicular to the orbital plane. Next, let $\bar{\rho}$ denote the position vector of the follower spacecraft relative to the leader spacecraft. In addition, let $\bar{\rho} = x\hat{i} + y\hat{j} + z\hat{k}$ and $\bar{\omega} = \omega\hat{k}$ be the vector representations of $\bar{\rho}$ and $\bar{\omega}$, respectively, in the moving reference x-y-z. Then, it follows from Refs. 2 and 10 that the linearized dynamic equations governing the motion of the follower spacecraft relative to the leader spacecraft are given by

$$\ddot{x} - 2\omega\dot{y} = F_x \tag{1}$$

$$\ddot{y} + 2\omega\dot{x} - 3\omega^2 y = F_y \tag{2}$$

$$\ddot{z} + \omega^2 z = F_z \tag{3}$$

where F_i, $i = x, y, z$, is the ith component of the resultant specific external disturbance and/or specific control force (i.e., force per unit mass) acting on the relative motion dynamics.

Equations (1–3) are known as the C-W equations and were originally derived in the context of the spacecraft rendezvous problem.[9] References 2 and 10 have shown that the open-loop spacecraft relative position dynamics are inherently unstable, and in the absence of any control input, a nonzero initial condition or a nonzero exogenous disturbance will cause the two spacecraft to drift apart with the passage of time.

Next, to design pulse-based, discrete-time controllers that accomplish the spacecraft formation flying objective, we begin with a continuous-time, state-space description of Eqs. (1–3). Thus, we define the state variables $x_1 \triangleq x$, $x_2 \triangleq \dot{x}$, $x_3 \triangleq y$, $x_4 \triangleq \dot{y}$, $x_5 \triangleq z$, and $x_6 \triangleq \dot{z}$. Using these state variables and observing the fact that the in-plane (x-y) dynamics are decoupled from the out-of-plane (z) dynamics, the state-space description for the combined in-plane and out-of-plane dynamics is given by

$$\dot{\boldsymbol{x}}(t) = \begin{bmatrix} A_1(\omega) & 0_{4\times 2} \\ 0_{2\times 4} & A_2(\omega) \end{bmatrix} \boldsymbol{x}(t) + \begin{bmatrix} B_1 & 0_{4\times 1} \\ 0_{2\times 2} & B_2 \end{bmatrix} u(t) \tag{4}$$

where $\boldsymbol{x} \triangleq [x_1\ \ x_2\ \ x_3\ \ x_4\ \ x_5\ \ x_6]^T$, $u \triangleq [u_x\ \ u_y\ \ u_z]^T$, and

$$A_1(\omega) \triangleq \begin{bmatrix} 0 & 1 & 0 & 0 \\ 0 & 0 & 0 & 2\omega \\ 0 & 0 & 0 & 1 \\ 0 & -2\omega & 3\omega^2 & 0 \end{bmatrix}, \qquad B_1 \triangleq \begin{bmatrix} 0 & 0 \\ 1 & 0 \\ 0 & 0 \\ 0 & 1 \end{bmatrix}$$

$$A_2(\omega) \triangleq \begin{bmatrix} 0 & 1 \\ -\omega^2 & 0 \end{bmatrix}, \qquad B_2 \triangleq \begin{bmatrix} 0 \\ 1 \end{bmatrix} \tag{5}$$

with u_i for $i = x, y, z$ being the control input.

Next, we obtain a sampled-data representation of the preceding continuous-time, state-space model of spacecraft relative position dynamics.[13] Thus, let T_1 and T_2 be the in-plane and out-of-plane sampling intervals, respectively, and define

$$A_{1d}(\omega) \triangleq e^{A_1(\omega)T_1}, \qquad B_{1d}(\omega) \triangleq \int_0^{T_1} e^{A_1(\omega)(T_1 - s)}\,\mathrm{d}s\,B_1$$

$$A_{2d}(\omega) \triangleq e^{A_2(\omega)T_2}, \qquad B_{2d}(\omega) \triangleq \int_0^{T_2} e^{A_2(\omega)(T_2 - s)}\,\mathrm{d}s\,B_2$$

With the preceding notation the combined in-plane and out-of-plane sampled-data spacecraft relative position dynamics are given by

$$\boldsymbol{x}(k+1) = \begin{bmatrix} A_{1d}(\omega) & 0_{4\times 2} \\ 0_{2\times 4} & A_{2d}(\omega) \end{bmatrix} \boldsymbol{x}(k) + \begin{bmatrix} B_{1d}(\omega) & 0_{4\times 1} \\ 0_{2\times 2} & B_{2d}(\omega) \end{bmatrix} u(k) \tag{6}$$

where $\boldsymbol{x}(k) \triangleq [x_1(kT_1)\ \ x_2(kT_1)\ \ x_3(kT_1)\ \ x_4(kT_1)\ \ x_5(kT_2)\ \ x_6(kT_2)]^T$, $u(k) \triangleq [u_1(kT_1)\ \ u_2(kT_1)\ \ u_3(kT_2)]^T$, etc.

III. Linear Pulse Control

As discussed earlier, a number of advanced pulse-type actuation technologies are currently being developed for spacecraft propulsion. Furthermore, it appears that, at least for the Earth-centric MSFF missions, it is wiser to exploit Kepler than to fight Kepler.[15] Thus, the various leader and follower spacecraft in the cluster of cooperative spacecraft can be typically parked in their natural orbits between useful mission operation periods. Next, for useful mission operation, the participating spacecraft can achieve the desired formation while still in their natural orbits. However, to extend the formation life for each cycle, it will be necessary to provide control thrust to mitigate the destabilizing influence of gravitational perturbation, differential drag, solar pressure disturbance, etc. In this section we develop pulse-based controllers that utilize continuous thrusting, for possibly short intervals, to achieve and maintain the formation configuration. The proposed pulse-based control design methodology is outlined next.

Consider the time-invariant, pulse-based, discrete-time feedback control system

$$\boldsymbol{x}(k+1) = \Phi\boldsymbol{x}(k) + \Gamma u(k), \qquad k = 0, 1, \ldots \tag{7}$$

$$\begin{aligned} u(k) &= K\boldsymbol{x}(k), && k = nN, \ldots, nN + p - 1 \\ &= 0, && k = nN + p, \ldots, nN + p + q - 1 \end{aligned} \tag{8}$$

where $\boldsymbol{x}$ is the system state vector, u is the control input vector, Φ is the system dynamic matrix, Γ is the input matrix, $n = 0, 1, 2, \ldots$, and $N = p + q$ is the number of samples in one complete cycle over which the control is first turned on for p samples and then off for the remaining q samples. In this case using a recursive solution procedure, it can be shown that

$$\boldsymbol{x}(nN) = [\Phi^q(\Phi + \Gamma K)^p]^n \boldsymbol{x}(0), \qquad n = 0, 1, 2, \ldots \tag{9}$$

The stability of the closed-loop system (7), (8) can be guaranteed by requiring that the solution of Eq. (9) decay. To this end, it follows that for the case when $p = 1$ Eq. (9) can be rewritten as

$$\boldsymbol{x}(nN) = \left[(\Phi^{(q+1)} + \Phi^q\Gamma K)\right]^n \boldsymbol{x}(0), \qquad n = 0, 1, 2, \ldots \tag{10}$$

To ensure that the solutions of Eq. (10) decay, we require that $\Phi^{(q+1)} + \Phi^q\Gamma K$ be asymptotically stable. When the pair $[\Phi^{(q+1)}, \Phi^q\Gamma]$ is stabilizable, this condition can be satisfied by designing the feedback gain K, for example, using the LQ control design technique.[16] Alternatively, one can use the standard pole placement algorithms[13] to design K such that

$$\rho\left(\Phi^{(q+1)} + \Phi^q\Gamma K\right) < 1 \tag{11}$$

where $\rho(X)$ is the spectral radius of a square matrix X (i.e., the maximum absolute value among all eigenvalues of X).

Next, for the pulse-based LQ control of Eq. (7), consider the stabilizable auxiliary system

$$\boldsymbol{z}(k+1) = \hat{\Phi}\boldsymbol{z}(k) + \hat{\Gamma}v(k) \tag{12}$$

where $z(k)$ and $v(k)$ correspond to the state and control, respectively, of the auxiliary system $\hat{\Phi} \triangleq \Phi^{(q+1)}$ and $\hat{\Gamma} \triangleq \Phi^q \Gamma$. Now design

$$v(k) = Kz(k) \tag{13}$$

that satisfies the following design criteria: 1) the closed-loop system (12), (13) is globally asymptotically stable and 2) the quadratic performance functional

$$J(K) \triangleq \sum_{k=0}^{\infty} z^T(k) R_1 z(k) + v^T(k) R_2 v(k) \tag{14}$$

where R_1 is a nonnegative-definite, state weighting matrix and R_2 is a positive-definite, control weighting matrix,[16] is minimized. It follows from Eq. (11) that the state feedback controller gain K that stabilizes the auxiliary closed-loop system (12), (13) also stabilizes the pulse-based, state feedback control system (7), (8). Thus, we now determine the pulse-based, state feedback control gain K by designing an LQ state feedback gain K for the auxiliary system. Finally, note the case when $p > 1$ is significantly more involved and can be addressed by replacing the time-invariant, state feedback controller (8) by a periodic, state feedback controller. This issue will be addressed in a future paper.

IV. Illustrative Numerical Simulations

In this section we provide illustrative numerical simulations to demonstrate the proposed pulse-based, discrete-time, linear control scheme for the relative position control of two spacecraft. The problem data are adopted from Ref. 2. Consider a leader-follower satellite pair to be in the geosynchronous orbit of radius $r = 42{,}241$ km. Let the orbital period be 24 h, thus $\omega = 7.2722 \times 10^{-5}$ radians/s. The control objective is to regulate the relative x position component to 100 m, the relative y and z position components to zero, and the relative x, y, and z velocities to zero with the in-plane control (u_x, u_y) and the out-of-plane control u_z applied 1 h and 4 h, respectively. The in-plane control and the out-of-plane control are each turned on for a 2 min duration at the beginning of their respective cycles. The control gains for the in-plane and out-of-plane dynamics are designed using the standard LQ regulation method with quadratic performance criteria[16]

$$J_{\text{ip}} = \sum_{k=0}^{\infty} z_1^2(k) + \frac{1}{\omega^2}\left[v_x^2(k) + v_y^2(k)\right] \tag{15}$$

$$J_{\text{op}} = \sum_{k=0}^{\infty} z_5^2(k) + \frac{1}{\omega^2} v_z^2(k) \tag{16}$$

where z_i and v_i are transformations of $\boldsymbol{x}_i$ and u_i to the auxiliary coordinate system described in Sec. III. For convenience, we scale the time units in Eqs. (4), (5), (15), and (16) from seconds to minutes. This is accomplished by replacing ω by $\hat{\omega} = 60\omega$. Now we design the in-plane state feedback gain K_{ip} using $[\hat{\Phi}_1(\hat{\omega}), \hat{\Gamma}_1(\hat{\omega})]$ and the quadratic performance criterion (15) where $\hat{\Phi}_1(\hat{\omega}) \triangleq [A_{1d}(\hat{\omega})]^{(q+1)}$, $\hat{\Gamma}_1(\hat{\omega}) \triangleq [A_{1d}(\hat{\omega})]^q B_{1d}(\hat{\omega})$, $T_1 = 2$ min and $q = 29$. In addition, we design the out-of-plane state feedback gain K_{op} using $[\hat{\Phi}_2(\hat{\omega}), \hat{\Gamma}_2(\hat{\omega})]$ and the quadratic performance criterion (16) where $\hat{\Phi}_2(\hat{\omega}) \triangleq [A_{2d}(\hat{\omega})]^{(q+1)}$, $\hat{\Gamma}_2(\hat{\omega}) \triangleq [A_{2d}(\hat{\omega})]^q B_{2d}(\hat{\omega})$, $T_2 = 2$ min and $q = 119$. The system response to nonzero initial condition $\boldsymbol{x}(0) = [200\ \ 0\ \ -100\ \ 0_{3\times 1}]^T$ and periodic solar pressure differential described in Refs. 2 and 10 (with appropriate time scaling to minutes) is given in Fig. 1. Unlike the unstable response in Refs. 2 and 10 for the open-loop system, the closed-loop response in Fig. 1 is bounded. However, the system response in Fig. 1 represents oscillatory behavior. This is because the system is subjected to periodic solar pressure differential, and the pulse-based controller is unable to reject the periodic disturbance. If the solar pressure differential is assumed to be absent, the closed-loop response asymptotically tracks the desired set point.

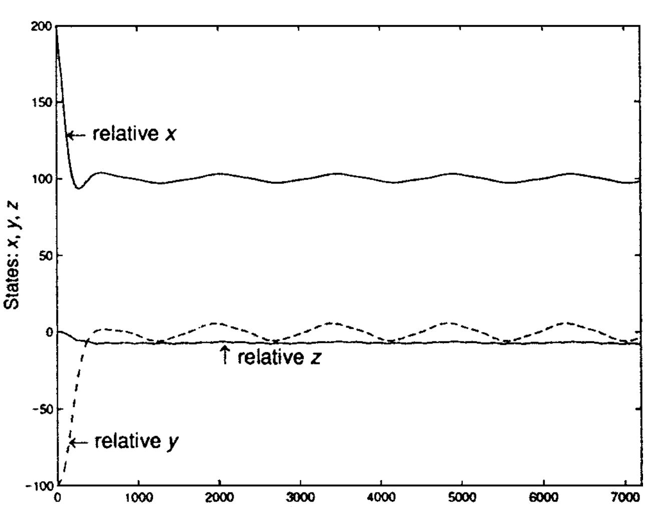

Fig. 1 Pulse-based spacecraft relative position control.

V. Conclusion

In this Note we developed a mathematically rigorous control design framework for linear control of spacecraft relative position dynamics with guaranteed closed-loop stability. In particular, a pulse-based control architecture has been proposed that can potentially lower the fuel consumption in MSFF. An illustrative numerical simulation demonstrated the efficacy of the proposed approach. Future work will consider generalization of the pulse-based, discrete-time feedback control law to the case $p > 1$ via a periodic control architecture.

Acknowledgments

Research supported in part by the Air Force Office of Scientific Research under the Summer Faculty Research Program and Grant F49620-93-C-0063, the Air Force Research Lab/VAAD, Wright–Patterson Air Force Base, Ohio under IPA; Visiting Faculty Grant, the NASA/New York Space Grant Consortium under Grant 32310-5891, and the Mechanical Engineering Department, Polytechnic University. The first author is grateful to the Air Force Research Laboratory, AFRL/VAAD at the Wright–Patterson Air Force Base for their hospitality during the summers of 1998 and 1999. In addition, he is indebted to Siva Banda of AFRL/VAAD, who introduced him to the problem of MSFF.

References

[1] Bauer, F., et al., "Satellite Formation Flying Using an Innovative Autonomous Control System (AUTOCON) Environment," *Proceedings of the AIAA Guidance, Navigation, and Control Conference*, AIAA, Reston, VA, 1997, pp. 657–666.

[2] Vassar, R. H., and Sherwood, R. B., "Formationkeeping for a Pair of Satellites in a Circular Orbit," *Journal of Guidance, Control, and Dynamics,* Vol. 8, No. 2, 1985, pp. 235–242.

[3] Redding, D. C., Adams, N. J., and Kubiak, E. T., "Linear-Quadratic Stationkeeping for the STS Orbiter," *Journal of Guidance, Control, and Dynamics,* Vol. 12, No. 2, 1989, pp. 248–255.

[4] Lau, K., Colavita, M., Blackwood, G., Linfield, R., Shao, M., and Gallagher, D., "The New Millennium Formation Flying Optical Interferometer," *Proceedings of the AIAA Guidance, Navigation, and Control Conference*, AIAA, Reston, VA, 1997, pp. 650–656.

[5] Guinn, J. R., "Autonomous Navigation for the New Millennium Program Earth Orbiter 1 Mission," *Proceedings of the AIAA Guidance, Navigation, and Control Conference*, AIAA, Reston, VA, 1997, pp. 612–617.

[6] "Shuttle 7 to Fly Approaches to Payload," *Aviation Week and Space Technology*, Vol. 118, No. 19, 1983, pp. 51–57.

[7] Wang, P. K. C., and Hadaegh, F. Y., "Coordination and Control of Multiple Microspacecraft Moving in Formation," *Journal of Astronautical Sciences*, Vol. 44, No. 3, 1996, pp. 315–355.

[8] Chobotov, V. A. (ed.), *Orbital Mechanics*, AIAA, Reston, VA, 1996, pp. 31–33.

[9] Clohessy, W. H., and Wiltshire, R. S., "Terminal Guidance System for Satellite Rendezvous," *Journal of Aerospace Science*, Vol. 27, No. 9, 1960, pp. 653–658.

[10] Kapila, V., "Spacecraft Formation Flying: A Survey," TR, Air Force Office of Scientific Research–Summer Faculty Research Program 1998, pp. 7.1–7.19.

[11] Leonard, C. L., Hollister, W. M., and Bergmann, E. V., "Orbital Formationkeeping with Differential Drag," *Journal of Guidance, Control, and*

Dynamics, Vol. 12, No. 1, 1989, pp. 108–113.

[12]Robertson, A., Corazzini, T., and How, J. P., "Formation Sensing and Control Technologies for a Separated Spacecraft Interferometer," *Proceedings of the American Control Conference*, 1998, pp. 1574–1579.

[13]Kuo, B. C., *Digital Control Systems*, Saunders HBJ, New York, 1992, pp. 55–59 and 556–566.

[14]Schilling, J., and Spores, R., "Comparison of Propulsion Options for TechSat 21 Mission," *Proceedings of the Air Force Research Laboratory–Formation Flying and Micro-Propulsion Workshop*, Air Force Research Lab., Elgin, FL, Oct. 1998.

[15]Vadali, S. R., "Analysis and Distributed Control of a Formation of Intelligent Satellites," *Proceedings of the Air Force Research Laboratory–Formation Flying and Micro-Propulsion Workshop*, Air Force Research Lab., Elgin, FL, Oct. 1998.

[16]Dorato, P., Abdallah, C., and Cerone, V., *Linear-Quadratic Control: An Introduction*, Prentice–Hall, Upper Saddle River, NJ, 1995, pp. 174–176.

Optimal Variable-Structure Control Tracking of Spacecraft Maneuvers

John L. Crassidis* and Srinivas R. Vadali†
Texas A&M University, College Station, Texas 77843-3141
and
F. Landis Markley‡
NASA Goddard Space Flight Center, Greenbelt, Maryland 20771

Introduction

IN recent years much effort has been devoted to the closed-loop design of spacecraft with large angle slews. Vadali and Junkins[1] and Wie and Barba[2] derive a number of simple control schemes using quaternion and angular velocity (rate) feedback. Other full-state feedback techniques have been developed that are based on variable-structure (sliding-mode) control, which uses a feedback linearizing technique and an additional term aimed at dealing with model uncertainty. A variable-structure controller has been developed for the regulation of spacecraft maneuvers using a Gibbs vector parameterization,[3] a modified-Rodrigues parameterization,[4] and a quaternion parameterization.[5] In both Refs. 2 and 5 a term was added so that the spacecraft maneuver follows the shortest path and requires the least amount of control torque. The variable-structure control approach using a quaternion parameterization has been recently expanded to the attitude tracking case.[6,7] However, these controllers do not take into account the shortest possible path as shown in Refs. 2 and 5.

This Note expands upon the results in Ref. 5 to provide an optimal control law for asymptotic tracking of spacecraft maneuvers using variable-structure control. It also provides new insight using a simple term in the control law to produce a maneuver to the reference attitude trajectory in the shortest distance. Controllers are derived for either external torque inputs or reaction wheels.

Background

In this section a brief review of the kinematic and dynamic equations of motion for a three-axis stabilized spacecraft is shown. The attitude is assumed to be represented by the quaternion, defined as $\boldsymbol{q} \equiv [\boldsymbol{q}_{13}^T \;\; q_4]^T$ with $\boldsymbol{q}_{13} \equiv [q_1 \;\; q_2 \;\; q_3]^T = \hat{\boldsymbol{n}} \sin(\Phi/2)$ and $q_4 = \cos(\Phi/2)$, where $\hat{\boldsymbol{n}}$ is a unit vector corresponding to the axis of rotation and Φ is the angle of rotation. The quaternion kinematic equations of motion are derived by using the spacecraft's angular velocity ($\boldsymbol{\omega}$), given by

$$\dot{\boldsymbol{q}} = \tfrac{1}{2}\Omega(\boldsymbol{\omega})\boldsymbol{q} = \tfrac{1}{2}\Xi(\boldsymbol{q})\boldsymbol{\omega} \tag{1}$$

where $\Omega(\boldsymbol{\omega})$ and $\Xi(\boldsymbol{q})$ are defined as

$$\Omega(\boldsymbol{\omega}) \equiv \begin{bmatrix} -[\boldsymbol{\omega}\times] & \vdots & \boldsymbol{\omega} \\ \cdots\cdots & \vdots & \cdots \\ -\boldsymbol{\omega}^T & \vdots & 0 \end{bmatrix}, \qquad \Xi(\boldsymbol{q}) \equiv \begin{bmatrix} q_4 I_{3\times 3} + [\boldsymbol{q}_{13}\times] \\ \cdots\cdots\cdots\cdots \\ -\boldsymbol{q}_{13}^T \end{bmatrix} \tag{2}$$

and $I_{n\times n}$ represents an $n \times n$ identity matrix. The 3×3 dimensional matrices $[\boldsymbol{\omega}\times]$ and $[\boldsymbol{q}_{13}\times]$ are referred to as cross-product matrices because $\boldsymbol{a}\times\boldsymbol{b} = [\boldsymbol{a}\times]\boldsymbol{b}$ (see Ref. 8).

Because a three degree-of-freedom attitude system is represented by a four-dimensional vector, the quaternion components cannot be independent. This condition leads to the following normalization constraint $\boldsymbol{q}^T\boldsymbol{q} = \boldsymbol{q}_{13}^T\boldsymbol{q}_{13} + q_4^2 = 1$. Also, the error quaternion between two quaternions $\boldsymbol{q}$ and $\boldsymbol{q}_d$ is defined by

$$\boldsymbol{\delta q} \equiv \begin{bmatrix} \boldsymbol{\delta q}_{13} \\ \cdots\cdots \\ \delta q_4 \end{bmatrix} = \boldsymbol{q} \otimes \boldsymbol{q}_d^{-1} \tag{3}$$

where the operator $\otimes$ denotes quaternion multiplication (see Ref. 8 for details) and the inverse quaternion is defined by $\boldsymbol{q}_d^{-1} = [-q_{d_1} \;\; -q_{d_2} \;\; -q_{d_3} \;\; q_{d_4}]^T$. Other useful identities are given by $\boldsymbol{\delta q}_{13} = \Xi^T(\boldsymbol{q}_d)\boldsymbol{q}$ and $\delta q_4 = \boldsymbol{q}^T\boldsymbol{q}_d$. Also, if Eq. (3) represents a small rotation, then $\delta q_4 \approx 1$ and $\boldsymbol{\delta q}_{13}$ corresponds to the half angles of rotation.

The dynamic equations of motion, also known as Euler's equations, for a rotating spacecraft are given by

$$J\dot{\boldsymbol{\omega}} = -\boldsymbol{\omega}\times(J\boldsymbol{\omega}) + \boldsymbol{u} \tag{4}$$

where J is the inertia matrix of the spacecraft and $\boldsymbol{u}$ is the total external torque input. If the spacecraft is equipped with three orthogonal reaction or momentum wheels, then Euler's equations become

$$(J - \bar{J})\dot{\boldsymbol{\omega}} = -\boldsymbol{\omega}\times(J\boldsymbol{\omega} + \bar{J}\bar{\boldsymbol{\omega}}) - \bar{\boldsymbol{u}} \tag{5a}$$

$$\bar{J}(\dot{\bar{\boldsymbol{\omega}}} + \dot{\boldsymbol{\omega}}) = \bar{\boldsymbol{u}} \tag{5b}$$

where $\bar{J}$ is the diagonal inertia matrix of the wheels, J now includes the mass of the wheels, $\bar{\boldsymbol{\omega}}$ is the wheel angular velocity vector relative to the spacecraft, and $\bar{\boldsymbol{u}}$ is the wheel torque vector.

Selection of Switching Surfaces

Optimal Control Analysis

We first consider a sliding manifold for a purely kinematic relationship, with $\boldsymbol{\omega}$ as the control input. The variable-structure control design is used to track a desired quaternion $\boldsymbol{q}_d$ and corresponding angular velocity $\boldsymbol{\omega}_d$. As shown previously for regulation,[5] under ideal sliding conditions the trajectory in the state space moves on the sliding manifold. For tracking the following loss function is minimized to determine the optimal switching surfaces:

$$\Pi(\boldsymbol{\omega}) = \frac{1}{2}\int_{t_s}^{\infty} \left[\rho\,\boldsymbol{\delta q}_{13}^T\boldsymbol{\delta q}_{13} + (\boldsymbol{\omega} - \boldsymbol{\omega}_d)^T(\boldsymbol{\omega} - \boldsymbol{\omega}_d)\right]\mathrm{d}t \tag{6}$$

subject to the bilinear system constraint given in Eq. (1). Note that ρ is a scalar gain and t_s is the time of arrival at the sliding manifold. Minimization of Eq. (6) subject to Eq. (1) leads to the following two-point-boundary-value problem:

$$\dot{\boldsymbol{q}} = \tfrac{1}{2}\Xi(\boldsymbol{q})\boldsymbol{\omega} \tag{7a}$$

$$\dot{\boldsymbol{\lambda}} = -\rho\,\Xi(\boldsymbol{q}_d)\Xi^T(\boldsymbol{q}_d)\boldsymbol{q} + \tfrac{1}{2}\Xi(\boldsymbol{\lambda})\boldsymbol{\omega} \tag{7b}$$

where λ is the costate vector. The optimal $\boldsymbol{\omega}$ is given by

$$\boldsymbol{\omega} = -\tfrac{1}{2}\Xi^T(\boldsymbol{q})\boldsymbol{\lambda} + \boldsymbol{\omega}_d \tag{8}$$

Received 26 April 1999; revision received 30 November 1999; accepted for publication 27 January 2000.

*Assistant Professor, Department of Aerospace Engineering. Senior Member AIAA.

†Professor, Department of Aerospace Engineering. Associate Fellow AIAA.

‡Engineer, Code 571, Guidance, Navigation, and Control Center. Fellow AIAA.